Available online at www.sciencedirect.com

SCIENCE DIRECT

Surface & Coatings Technology 200 (2006) 2672–2678

SURFACE & COATINGS TECHNOLOGY

www.elsevier.com/locate/surfcoat

The effect of N^+-implanted aluminum substrate on the mechanical properties of TiN films

Youming Liu[a], Liuhe Li[a,b,*], Ming Xu[a], Qiulong Chen[a], Yawei Hu[a], Xun Cai[a], Paul K. Chu[c]

[a]*School of Material Science and Engineering, Shanghai Jiao Tong University, Shanghai 200030, China*
[b]*702 Department, Mechanical Engineering School of Beijing University of Aeronautic and Astronautic, 100083, China*
[c]*Department of Physics & Materials Science, City University of Hong Kong, Kowloon, Hong Kong*

Received 24 June 2004; accepted in revised form 31 December 2004
Available online 26 February 2005

Abstract

In this work, nitrogen ions were implanted into an aluminum sample prior to magnetron sputtering for deposition of TiN films by self-designed multifunction ion implanter. An 80 nm thick aluminum nitride (AlN) layer is observed by Auger Electron Spectrometer. We examine the effects of AlN layer on the surface mechanical properties of aluminum by nanoindentation. The effects of the AlN layer on the surface mechanical properties are evaluated. The hardness and elastic modulus of the TiN films on the two different substrates (N ion implanted and unimplanted) are almost constant in the near surface region and decrease with increasing indentation depths. A reduced rate of decrease in the hardness and modulus is observed in the TiN/N^+-implanted aluminum. From the results obtained by scratch test, the adhesion strength of TiN/N^+-implanted aluminum is better than TiN/unimplanted sample.

Keywords: TiN films; N^+-implanted aluminum; Nanohardness; Modulus; Adhesion strength

1. Introduction

Because of the light weight as well as high shearing strength, corrosion resistance, electrical conductivity and heat conductivity, aluminum alloys are widely used in the aerospace, electronic, and automobile industries [1,2]. However, the low hardness and wear resistance of aluminum and its alloys have hampered a wider application of the materials, particularly as load-bearing components and friction parts. Hence, it is necessary to improve the surface properties of aluminum and its alloy. Among the possible surface treatment techniques, nitrogen ion implantation has been proposed [3–6]. In this way, an aluminum nitride (AlN) layer is formed and previous studies have shown that the nanohardness and frictional properties of aluminum can be improved. However, the implanted layer thickness is too thin (usually around 100 nm) [4] and it is insufficient against wear and tear for many applications in the field. TiN possesses good wear and corrosion resistance and has been used as a hard coating in applications such as cutting tools and the microelectronic industry. In the work described here, we deposit TiN films on nitrogen implanted aluminum alloy to increase the protecting layer thickness. One of our objectives is to improve the adhesion between the TiN and Al substrate. Conventionally, it is accomplished by the deposition of a Ti interlayer on the substrate before the TiN coating is deposited. Here, we propose an alternative method by using nitrogen ion implantation to generate the buffer layer that can spread the stress gradually. It is expected to enhance the resistance against large loading and plastic deformation.

2. Experimental procedures

Samples 15×15×5 mm made of pure aluminum (99.99%) were used in our experiments. The samples were

* Corresponding author. School of Material Science and Engineering, Shanghai Jiao Tong University, Shanghai 200030, China.
E-mail address: Liuhena@vip.sina.com (L. Li).

0257-8972/$ - see front matter © 2005 Elsevier B.V. All rights reserved.
doi:10.1016/j.surfcoat.2004.12.030

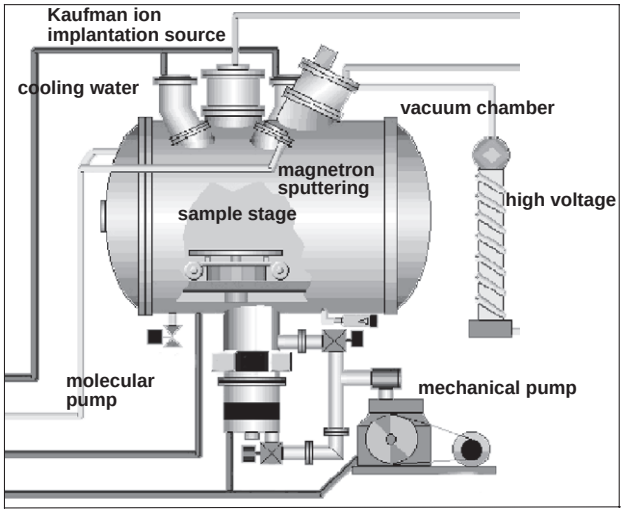

Fig. 1. Schematic of custom-designed multi-functional ion implanter.

mechanically polished and ultrasonically cleaned in isopropyl alcohol for about 10 min prior to implantation. Ion implantation was conducted in a custom-designed multi-functional ion implanter schematically depicted in Fig. 1. The instrument is equipped with a DC magnetron sputtering source and a Kaufman ion implantation source in the same vacuum chamber. The sample temperature during implantation was measured by a thermocouple mounted on the sample holder and a pyrometer installed in the vacuum chamber. No external heating was applied to the specimen and so any temperature increase was due to the incident ion implantation and magnetron sputtering process. The sample was implanted with 30 kV N_2^+ ions to a dose of 1×10^{17} cm^{-2}. The ion beam current density was ~25 μA/cm^2.

After implantation, the sample was moved to the magnetron sputtering source without breaking vacuum. The background pressure in the deposition chamber was less than 2×10^{-3} Pa. The distance between the sample and magnetron sputtering source was about 4 to 5 cm. The target was made of 99.4% pure titanium, and the target voltage and current were 420 V and 1.0 A, respectively. The nitrogen and argon gases were 99.99% pure, and the total pressure and N_2 partial pressure were 3.0×10^{-1} Pa and 5.0×10^{-2} Pa, respectively. The thickness of the TiN films was determined by profilometry and the deposition rate was calculated to be ~0.47 nm/s; nitrogen depth profiles were obtained by Auger electron spectrometry using a sputtering rate of 7 nm/min. The critical load of adherence was determined using a micro-scratch tester (CSEM Instruments), provided with an automatic displacement of the sample under the Rockwell diamond indenter (200 μm radius) at a approach speed velocity of 0.2%/s and with a loading rate of 5 N/s. The scratch channel was observed under a 200× microscope to determine the critical load, which was associated with the first observable failure of the coating.

2.1. Depth profiles

The O, Al, N depth profiles acquired from the 30 kV, 1×10^{17} N_2^+/cm^2 sample are displayed in Fig. 2. The N profile resembles a roughly Gaussian profile with a maximum nitrogen concentration 40 at.% at a depth of 40 nm and some diffusion to a depth of 80 nm. The Al profile shows a concentration of 20.5 at.% on the surface that increases with depth and the substrate is reached at 80 nm. The implanted layer is believed to consist of metallic aluminum and AlN precipitates [7]. At the surface of the unimplanted aluminum, stoichiometric Al_2O_3 is observed [8] and the oxygen concentration decreases with increasing nitrogen concentration. Refs. [7,8] show very small carbon

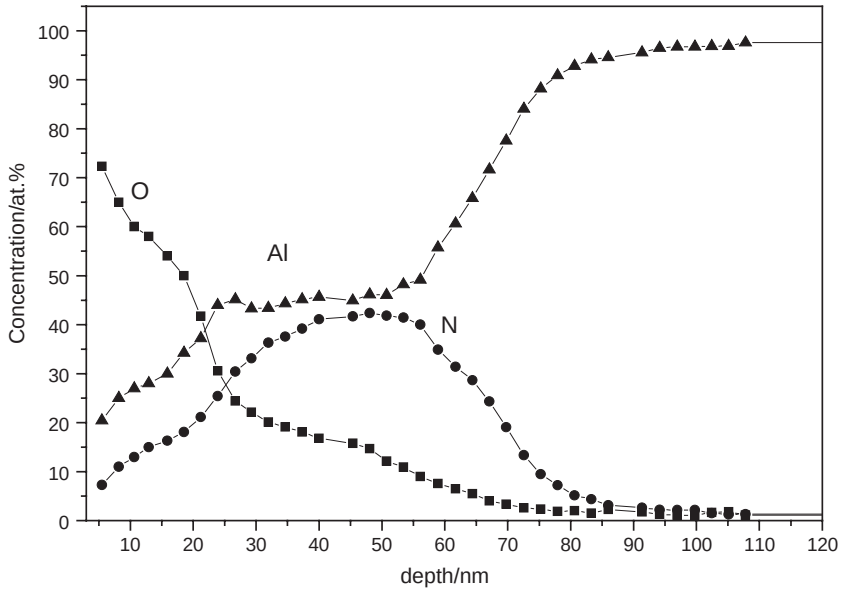

Fig. 2. Depth profiles of Al, N, O in the implanted sample.

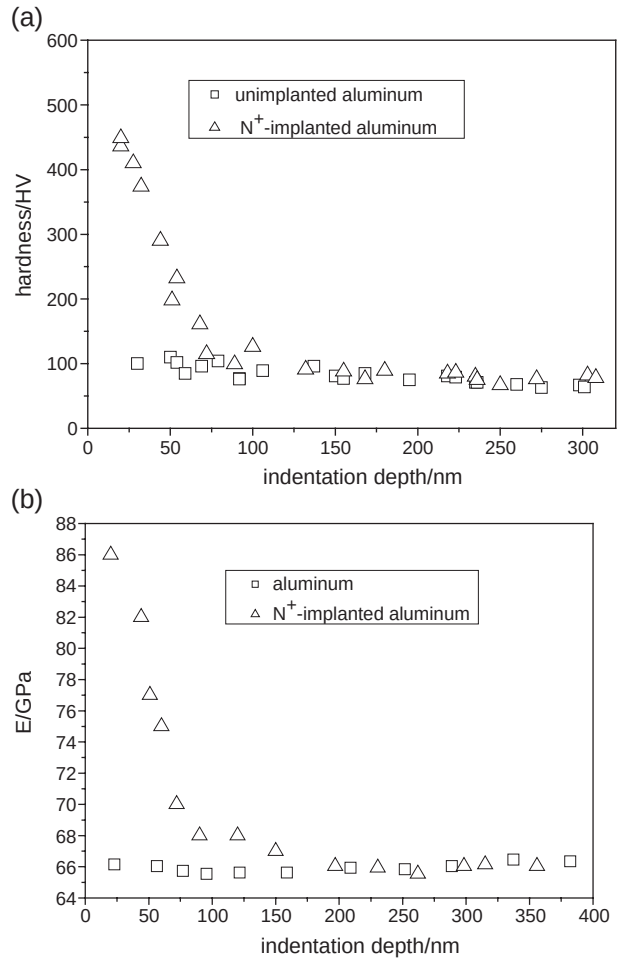

Fig. 3. Nanohardness (a) and elastic modulus (b) of N^+-implanted aluminum and unimplanted aluminum as a function of the indentation depth.

contamination in the implanted samples probably due to hydrocarbon adsorption on the surface, but in our experiments, only the three major elements could be measured up to the detection limits of AES.

2.2. Nanoindentation test

A plot of the nanohardness and elastic modulus as a function of the indentation depth of the N^+-implanted and unimplanted aluminum is shown in Fig. 3. A series of indentations were made to depths ranging from 20 to 300 nm depending on the load. The compound hardness calculated using the method of Oliver and Pharr is shown in Fig. 3(a). Each data point represents an average of five indentations. For the N^+-implanted sample, the hardness at 20 nm is 450 HV, where the applied maximum load is 0.1 mN. The hardness is observed to decrease with increasing depth of indentation in the near surface region and then has a constant value of 65 HV afterwards. In order to measure the "film-only" properties, a commonly used rule of thumb is to limit the indentation depth to less than 10% of the thickness [9,10]. In this work, the thickness of AlN layer ("film") is about 80 nm, and consequently, the indentation depth must be less than 8 nm. However, the minimum indentation depth of N^+-implanted sample is 20 nm. Therefore, the hardness values combine the effect of implantation and the underlying substrate. Because aluminum is very soft, the real hardness of the implanted layer is higher than the measured value. An increase in hardness is to be expected but only at a smaller load. In this work, however, the load of nanoindenter is limited to 0.1–300 mN. For the unimplanted sample, a compact amorphous Al_2O_3 layer with typically 5 nm thick grows on Al when it is exposed to air [11,12]. Therefore, the hardness is almost constant at practically all the indentation depths. Fig. 3(b) shows the Young's moduli of the N^+-implanted and unimplanted aluminum determined using the method of Oliver and Pharr. The composite modulus of the N^+-implanted aluminum is around 86 GPa at extremely small depths (20 nm) and then significantly decreases with increasing depth of indentation. Chudoba [13] suggests that it is very difficult to measure the correct modulus of films with a thickness less than 0.5 μm with Berkovich or Vicker indenter, because the contact depths are required below 10–15 nm. In this work, the minimum contact depth is 20 nm

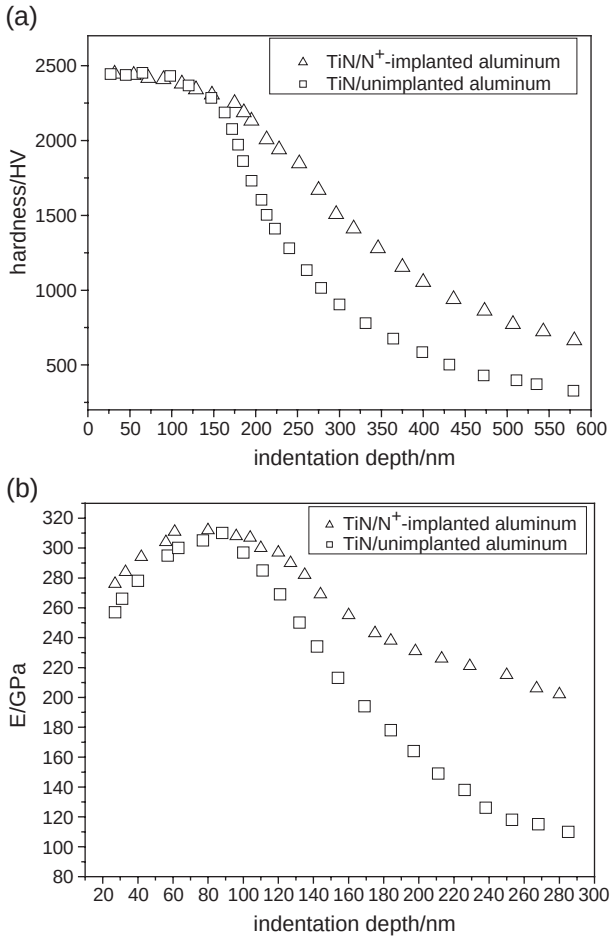

Fig. 4. Hardness (a) and elastic modulus (b) of TiN film on different substrate plotted as a function of indentation depth.

due to the limitation of indenter. So the measured modulus reflects the composite information of film and substrate. For the bulk aluminum substrate, the modulus is relatively constant.

Fig. 4 compares the hardness and elastic modulus of the 1700 nm TiN film on the two different substrates (implanted and unimplanted). The results are plotted as a function of the indentation depth. Fig. 4(a) shows the hardness calculated using the method of Oliver and Pharr [9]. It can be observed that the hardness of the TiN/implanted aluminum within the top 200 nm is between 2200 HV and 2400 HV and then decreases to 1420 HV at 300 nm. The hardness for the case of TiN on unimplanted aluminum in the top 200 nm is almost the same as that of TiN on implanted aluminum, although the rate of decline is larger than the TiN/implanted aluminum. Fig. 4(b) is a plot of the Young's moduli of the 1700 nm TiN film on different substrates. The modulus of the film within the top 80 nm increases slightly from 274 to 311 GPa and then decreases with increasing depth of indentation. The probable reason for this is that a larger stress concentrates in the TiN film in the near surface, and the load spreads the stress to the substrate. Similar results have been observed by Ranjana [14]. Again, the larger rate of decrease is observed in the TiN/unimplanted aluminum. Since the substrate is very soft compared to the film, it yields when the indentation depth is more than 10% the film thickness. The difference in hardness and thermal expansion coefficient between the TiN film and aluminum substrate is extremely large, and it leads to large residual stress between the film and substrate.

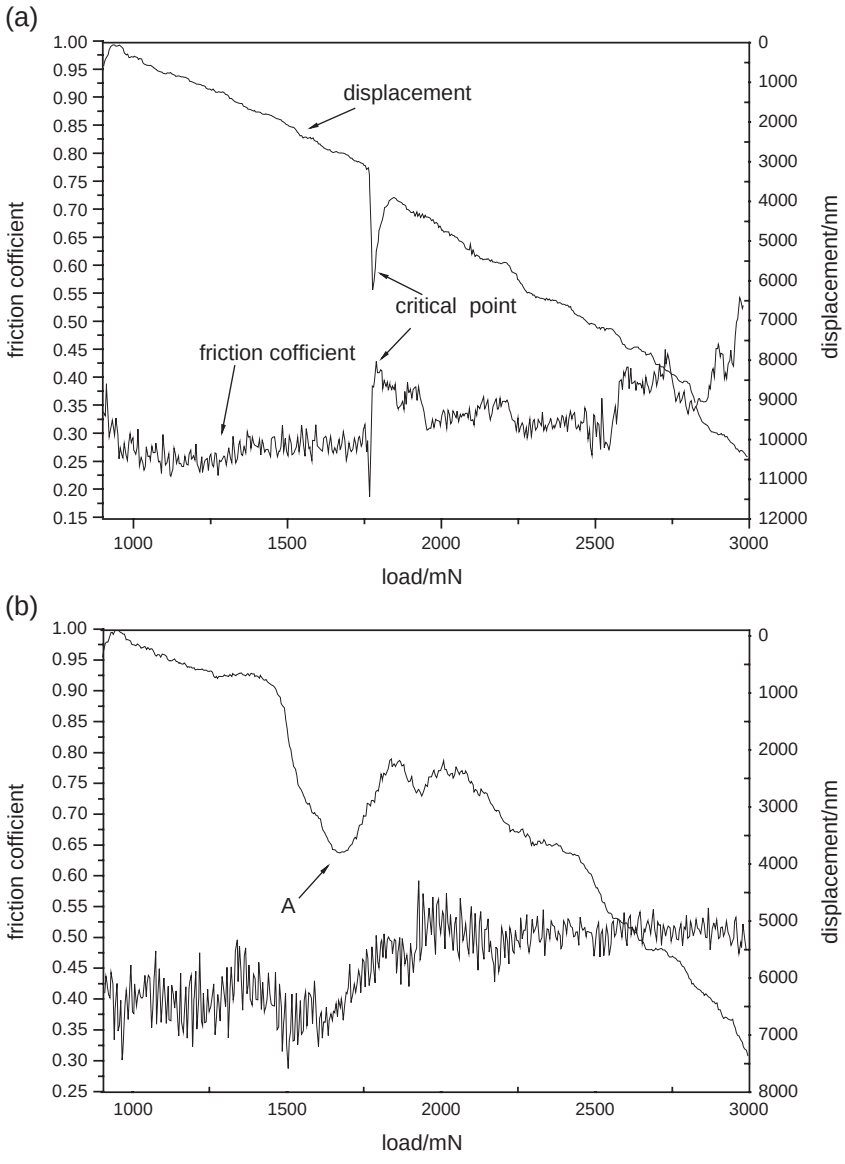

Fig. 5. Friction coefficient and displacement into the sample as a function of applied load for TiN coating on different substrates, (a) TiN/N^+-implanted aluminum; (b) TiN/aluminum.

2.3. Scratch test

Fig. 5 shows the typical coefficient of friction and displacement into the TiN films on two different substrates as a function of load. It can be observed from Fig. 5(a) that the friction coefficient almost keeps constant as the applied load increases from 1 N to 1.78 N, and then fluctuate suddenly at 1.78 N. Meanwhile, the results are certified by 200× microphotos to identify the onset of cracking. The failure mechanisms for the TiN/N^+-implanted aluminum are shown in Fig. 6(a), (c), (e). Fig. 6(a) shows the scratch channel before 1.78 N, scratch channel is smooth and there is not crack observed. Fig. 6(c) shows a large asperity at 1.78 N. Fig. 6(e) shows cracks and fracture at 3 N, and there is slight spalling at the edge of scratch channel. It is explained that in the initial region, the hardening of the surfaces is taking place, in the second region, the interface cohesive stress is exceeded, the cracks ahead of the indenter propagate to form semi-circular cracks. When applying load further, either the brittle nature of the coating or the stored elastic energy is sufficient to cause spallation and fracture at the edge and in front of the indenter. Fig. 6(b) shows the case of TiN on unimplanted aluminum. In the initial region, the fluctuation of friction coefficient and displacement has happened. Although the most violent fluctuation occurs at 1.6 N, identified by microphotos of scratch channel showed in Fig. 6(b), (d), (f), the scratch channel for initial region has showed semi-circular cracks (Fig. 6(b)). When applied the 1.6 N pointed by arrow A in Fig. 5(b), the SEM of scratch channel shows serious spalling (Fig. 6(d)). The TiN film is peeled out the substrate at 3 N (Fig. 6(f)). Thus, we can conclude that the cohesion strength is less than 1 N. Ashrafizadeh [15] also reported that the critical load of PVD TiN films (5 μm) on aluminum substrate is 0.5 N. From the previous results, it seems that the decision of critical load of adhesion is complex: friction coefficient, displacement and SEM or microphoto of scratch channel should be considered comprehensively.

Hu [16] and Dyrda [17] suggest that the harder the coating is, the better its adhesion to the substrate. Hu [14] gives the relation between the critical shear stress for coating peeling and the critical load L_c yields as:

$$\tau_c = \sqrt{2} K H_s^{\frac{1}{2}} L_c^{\frac{1}{2}} / \left(\sqrt{\pi} R\right), \tag{1}$$

where H is the hardness of substrate, R the radius of spherical indenter, and K the coefficient in relation to

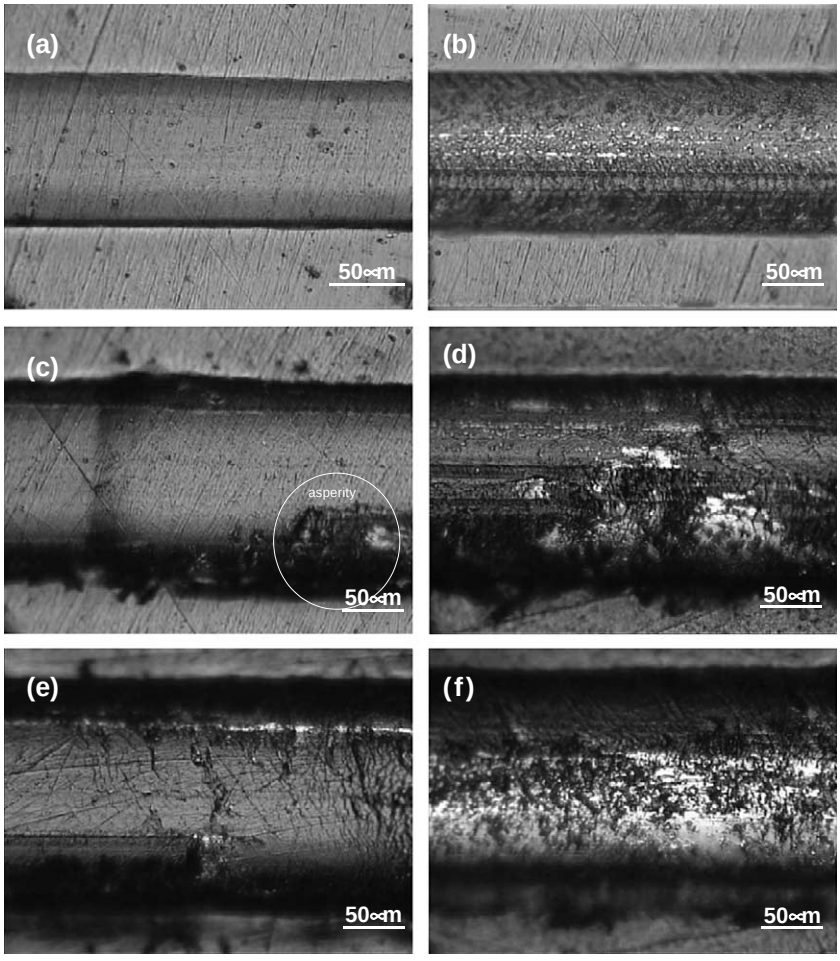

Fig. 6. The comparison of scratch channel of TiN on different substrate (a), (c), (e), TiN/N^+-implanted aluminum; (b), (d), (f), TiN/aluminum.

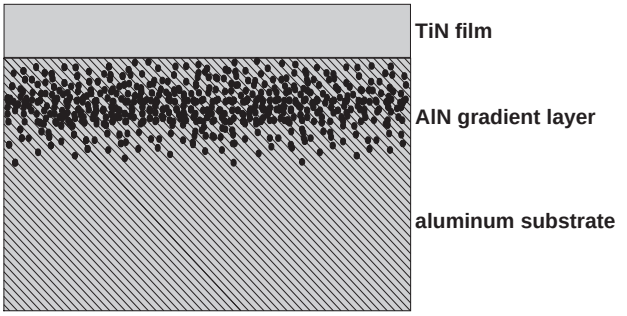

Fig. 7. Schematic of adhesion strengthening in the TiN/N^+-implanted aluminum.

friction. The critical shear stress for coating peeling increases with increasing load. After nitrogen implantation, the surface hardness of the substrate goes up from 100 HV to 450 HV. The substrate with higher hardness could provide a more effective support for the TiN film and thus the critical shear stress increases. The effect of the substrate on the mechanical properties of the thin film has been reported [16–19], and there are other reports [20,21] mentioning the effect of the interlayer on the mechanical properties of thin film, but the use of a gradient film without an obvious interface has not been reported based on our knowledge. In this work, the thickness of enhancement AlN layer is only 80 nm and it is easy for the AlN layer to yield, but the adhesion of TiN on N^+-implanted aluminum is improved effectively. The potential influencing factor will be discussed in the following paragraph.

Fig. 7 shows the schematic of adhesion strengthening in the TiN/implanted aluminum. After nitrogen implantation, the nitrogen atoms are distributed in aluminum roughly resembling a Gaussian and thus a gradient layer is also formed. Because the Young's moduli E of TiN and aluminum are quite different, the variation of stress is not continuous under loading. However, the AlN gradient layer possesses high hardness and high adhesion strength with the substrate, and so the stress is subjected to a gradient distribution. As a result, the ability to support loading and resist plastic deformation is improved. For TiN/N^+-implanted Al system, the Al substrate are heated by ion bombardment, radiations of arcs and atom collisions in the substrate during high energy ion implantation, and there is not cooling device attached to samples, hence the temperature of the samples is increased to about 200 °C, which is certified by Mitsuo [22]. The process temperature is the same for the magnetron sputtering TiN films on both substrates—implanted and unimplanted aluminum because of the same process parameter. Therefore, the process temperature of TiN/N^+-implanted Al system is much higher than that of TiN/unimplanted Al system. Higher temperature of substrate can improve the interdiffusion of films and substrate, thus, the adhesion strength between the TiN film and N^+-implanted aluminum substrate is improved. Solodukhin [21] and Hwang [23] also got the same conclusion. In addition, during ion implantation, surface contaminants and oxide film of aluminum substrate which decreases the adhesion strength of TiN films on substrate are removed, and high energy ion implantation causes radiation damages on the substrate surface that may be beneficial to nucleation. The observed enhancement is believed to stem from the combined synergistic effects.

3. Conclusions

(1) The surface properties of aluminum are improved by depositing TiN after nitrogen ion implantation to form a 80 nm thick AlN gradient layer. Comparison of the load–displacement curve of aluminum and N^+-implanted aluminum shows that the harder AlN layer increases the hardness value. For the unimplanted sample, the hardness is almost constant at all the indentation range.

(2) The hardness of the TiN/N^+-implanted aluminum within the top 200 nm is between 2200 HV and 2400 HV and then it decreases to 1420 HV at 300 nm. The hardness of TiN on aluminum within the top 200 nm is almost the same as TiN on implanted aluminum, but the rate of decline is larger than the TiN/implanted aluminum. Therefore, after nitrogen ion implanted to aluminum, the ability to support loading and resist plastic deformation is improved.

(3) Scratch tests show that critical load for TiN/N^+-implanted aluminum is 1.78 N, much better than TiN/aluminum.

Acknowledgements

This work was supported by National Natural Science Foundation of China No. 50271004, Scientific Effort of Shanghai Science and Technology Committee 0359nm005 and City University of Hong Kong Strategic Research Grant SRG #7001642.

References

[1] E.A. Starke Jr., J.T. Staley, Prog. Aerosp. Sci. 32 (1996) 131.
[2] P.K. Rohatgi, Fuel Energy Abstr. 39 (1998) 25.
[3] J. Jagielskia, A. Piatkowska, P. Aubert, C. Legrand-Buscema, Vacuum 70 (2003) 147.
[4] J. Chakraborty, S. Mukherjee, P.M. Raole, P.I. John, Mater. Sci. Eng., A 304–306 (2001) 910.
[5] H.K. Sanghera, J.L. Sullivan, S.O. Saied, Appl. Surf. Sci. 141 (1999) 57.
[6] Brian W. Karr, I. Petrov, David G. Cahill, J.E. Greene, Appl. Phys. Lett. 70 (1997) 1703.
[7] T. Reier, J.W. Schultze, W. Osterle, Ch. Buchal, Thin Solid Films 385 (2001) 29.
[8] V.V. Ugolv, A.P. Laskovnev, N.N. Cherenda, et al., Surf. Coat. Technol. 83 (1996) 296.
[9] W.C. Oliver, G.M. Pharr, J. Mater. Res. 7 (1992) 1564.

[10] N.G. Chechenin, J. Bottiger, J.P. Kroge, Thin Solid Films 261 (1995) 219.
[11] R. Checchetto, L.M. Gratton, A. Miotello, Surf. Coat. Technol. 158–159 (2002) 356.
[12] L.H. Milacek, R.D. Daniels, J.A. Cooley, J. Appl. Phys. 39 (1968) 2803.
[13] T. Chudoba, J. Mater. Res. 19 (2004) 301.
[14] Ranjana Saha, William D. Nix, Acta Mater. 50 (2002) 23.
[15] F. Ashrafizadeh, Surf. Coat. Technol. 130 (2000) 183.
[16] S.B. Hu, J.P. Tu, Z. Mei, Surf. Coat. Technol. 141 (2001) 174.
[17] Katia Dyrda, Michael Sayer, Thin Solid Films 355–356 (1999) 277.
[18] R. Saha, W.D. Nix, Mater. Sci. Eng., A 319–321 (2001) 898.
[19] G.S. Kim, S.Y. Lee, J.H. Hahn, et al., Surf. Coat. Technol. 171 (2003) 83.
[20] F.S. Shieu, L.H. Cheng, M.H. Shiao, S.H. Lin, Thin Solid Films 311 (1997) 138.
[21] I.A. Solodukhin, V.V. Khodasevicha, et al., Surf. Coat. Technol. 142–144 (2001) 1144.
[22] A. Mitsuo, S. Uchida, T. Aizawa, Surf. Coat. Technol. 186 (2004) 196.
[23] Un-Hak Hwang, Thin Solid Films 254 (1995) 16.